Available online at www.sciencedirect.com

ScienceDirect

Ceramics International 40 (2014) 3371–3377

CERAMICS INTERNATIONAL

www.elsevier.com/locate/ceramint

Luminescence of $LiNbO_3$ polycrystalline ceramics: Effect of Sc_2O_3 and Lu_2O_3 doping

Anil Tumuluri[a], K.C. James Raju[a,b,*]

[a]Advanced Centre of Research in High Energy Materials, University of Hyderabad, Hyderabad 500046, India
[b]School of Physics, University of Hyderabad, Hyderabad 500046, India

Received 29 July 2013; received in revised form 14 September 2013; accepted 22 September 2013
Available online 30 September 2013

Abstract

Sc_2O_3 and Lu_2O_3 doped $LiNbO_3$ polycrystalline ceramics were prepared by the solid state reaction method. Structural, morphological and luminescence properties have been studied by X-ray diffraction, Raman spectroscopy, FE-SEM and Flurospectrometery respectively. From XRD, no structural changes have been observed in Sc_2O_3 and Lu_2O_3 doped $LiNbO_3$. SEM images show clear and distinct grains. Strong violet luminescence at 414 nm and 435 nm were observed for all samples with excitation in UV region (370 nm). Apart from this, with excitation at 289 nm, blue emission at 473 nm in pure $LiNbO_3$ is observed. With change in Sc_2O_3 dopant concentration, this peak is red shifted to 505 nm and 525 nm exhibiting green emission. Changes observed in Raman modes strongly support Stokes shift in luminescence peaks. Sc_2O_3 and Lu_2O_3 doped $LiNbO_3$ can be used as an efficient luminescent material in violet, blue and green region under UV excitation.

Keywords: B. Defects; C. Optical properties; D. Niobates

1. Introduction

The contribution of ferroelectric, nonlinear-optic and piezoelectric properties of $LiNbO_3$ (LN) system made it interesting for many versatile engineering applications [1–4]. It is being synthesised in many forms like single crystal slices, polycrystalline thin films, powders and as bulk pellets. In these varied forms, they are exhibiting a wide range of properties suitable for applications in photonic, telecom and sensing [5–8]. In particular, studies on Rare-Earth (RE) ion doped LN is of great importance because of its excellent luminescence behaviour. Investigation of optical properties with trivalent RE ions like Pr^{3+}, Dy^{3+}, Ho^{3+}, Er^{3+}, Tb^{3+}, Nd^{3+} and Tm^{3+} in LN as host material is already reported [9]. Amidst RE ions, much work has been devoted for Er^{3+} as active ion in LN host. Er^{3+} ion has a distinctive energy level structure that enables it possible for LN to obtain efficient up converted emissions under different excitation wavelengths [10–11]. Lili Xing et.al [12], reported the luminescence properties of $Ho^{3+}/Yb^{3+}/Tm^{3+}$/LN polycrystals and found that up conversion of white light emission is possible which can be used for potential applications as a white light emitting device.

Trivalent RE ions like Lu^{3+} and Sc^{3+} has attracted many researchers because of its high physical and chemical stabilities. Sc_2O_3 with its attractive properties like bulk refractive index (1.90 at 400 nm) and a high UV cut-off (at 215 nm) is useful in many technological applications in the field of optical devices such as solid state lasers, luminescent displays and optical amplifiers [13–16]. Moreover, the photorefractive damage of $LiNbO_3$ can be avoided by co-doping with ZnO, MgO and Sc_2O_3 [17]. Lu_2O_3 is also a promising luminescent material for its use in design of white light emitting diodes. The high density of 9.4 g/cm^3 is also helpful in utilising it as an efficient matrix component to enhance the density and transparency of the host material [18]. Moreover the ionic radii of Lu^{3+} (0.977 Å) and Sc^{3+} (0.87 Å) are close to both

Abbreviations: LN, $LiNbO_3$

*Corresponding author at: Advanced Centre of Research in High Energy Materials, University of Hyderabad, Hyderabad 500046, India.
Tel.: +91 40 23134305; fax: +91 40 23010227.
E-mail address: kcjrsp@uohyd.ernet.in (K.C.J. Raju).

0272-8842/$ - see front matter © 2013 Elsevier Ltd and Techna Group S.r.l. All rights reserved.
http://dx.doi.org/10.1016/j.ceramint.2013.09.095

Li^{+}(0.92 Å) and Nb^{5+}(0.74 Å). Therefore, doping Lu^{3+} and Sc^{3+} may replace for either Li^{+} or Nb^{5+} in the host matrices. The variations obtained in the pure LN with Sc_2O_3 and Lu_2O_3 will be interesting in the field of luminescence.

In this manuscript, different wt% of Lu_2O_3 and Sc_2O_3 doped polycrystalline LN were prepared. LN doped with different wt% of Sc_2O_3 has emission spectra in the violet and green regions with two different excitation wavelengths (370 nm, 289 nm) in the UV region. Similarly, LN doped with Lu_2O_3 has emission spectra in the violet and blue region excited with two different wavelengths (370 nm, 307 nm) in the UV region. The luminescence properties obtained with Sc_2O_3 and Lu_2O_3-LN system exhibited a different trend with different wt% of doping. The effect of concentration on the quenching of luminescence is also explained. Thus, the present work enriches the efforts being made in the development of scandium and lutetium activated luminescent materials in the violet, blue and green wavelength regions.

2. Experimental

The mixture of LN powder (99.99%-Alfa Aesar), Li_2O (99.99%-Alfa Aesar), Lu_2O_3 (99.9%-Sigma Aldrich), and Sc_2O_3 (99.9%-Sigma Aldrich) was milled for 5 h with distilled water as mixing agent. Zirconia balls were used as milling media. 5 wt% of Li_2O was added in addition to compensate the Li loss. This mixture was dried at 90 °C for 12 h. Pellets of 12 mm diameter doped with different wt% $x=2$, 4, 6 and 8 ("x" represents dopant concentration) were pressed with PVA as a binder. These samples were heat treated for binder burnout at 500 °C at the rate of 1 °C/min for 2 h. After binder burnout, the samples were sintered at an optimised temperature of 1125 °C at the rate of 10 °C/min for 2 h.

The crystallisation phase has been identified using X-ray diffraction spectra measured by a BRUKER X-ray diffractometer using a copper Kα radiation source. Raman spectra for the same were measured at room temperature by Lab-Ram spectrometer with a magnification of 50× and resolution of 2 cm^{-1}, using 514.5 nm line of argon ion laser as excitation source.

Morphological characterisation was carried out by using a Carl Zeiss, Ultra 55 which is a Field Emission Scanning Electron Microscope (FE-SEM) coupled with Energy Dispersive Spectrometer (EDS). Photoluminescence studies were carried out using a Horiba Jobin Yvon model FL3-22 spectrometer.

3. Results and discussion

3.1. Structural analysis

Fig. 1(a) and (b) shows the XRD patterns of the Sc_2O_3 and Lu_2O_3 doped LN respectively (where $x=2$, 4, 6, 8 represents the wt%). Indexing of diffraction peaks for all the samples has been done based on the standard $LiNbO_3$ and Lu_2O_3 XRD pattern (JCPDS diffraction file # 20-0631 and 86-2475). From the patterns, it is revealed that the dopants Sc_2O_3 and Lu_2O_3 do not have not much influence on the structure. From this, it is speculated that doping ions Sc^{3+} and Lu^{3+} may have formed complete solid solutions with LN. In addition, two peaks at 28.9° and 30.5° arising from Lu_2O_3 were identified and encircled in Fig. 1(b).

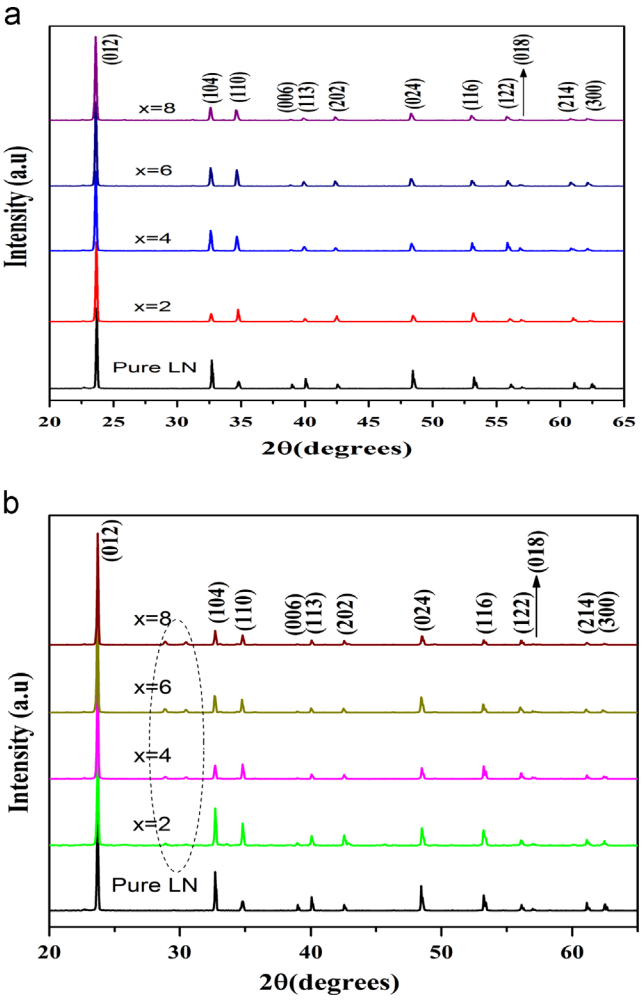

Fig. 1. (a) XRD for Sc_2O_3 doped LN. (b) XRD for Lu_2O_3 doped LN.

It is further noticed that the (006) peak of pure LN slowly disappeared with increase in dopant concentration. Usually, (006) peak in LN arises because of the grains oriented in *C*-axis. With increasing dopant concentration, the grain orientation in *C*-axis is disturbed. The ionic radius of Sc^{3+} (0.87 Å) is less than that of Li^{+} (0.92 Å) and is more than ionic radius of Nb^{5+} (0.74 Å). The increase in lattice parameter "*c*" and the expansion of unit cell volume represents the probability of occupying Nb^{5+} sites by Sc^{3+} rather than Li^{+} sites.

In case of Lu_2O_3, the ionic radius of Lu^{3+} (0.97 Å) is more than both Li^{+} (0.92 Å) and Nb^{5+} (0.74 Å). There is no consistent increase in cell volume and lattice parameter as in the case of Sc_2O_3. The possible reason may be due to lutetium, which partially reacted with host matrix LN resulting in an unsystematic increment of cell volume as shown in Table 2. This has been confirmed from peaks circled in Fig. 2 corresponding to Lu_2O_3. The variation in intensities of peaks (104) and (110) and lattice parameters attributed to the

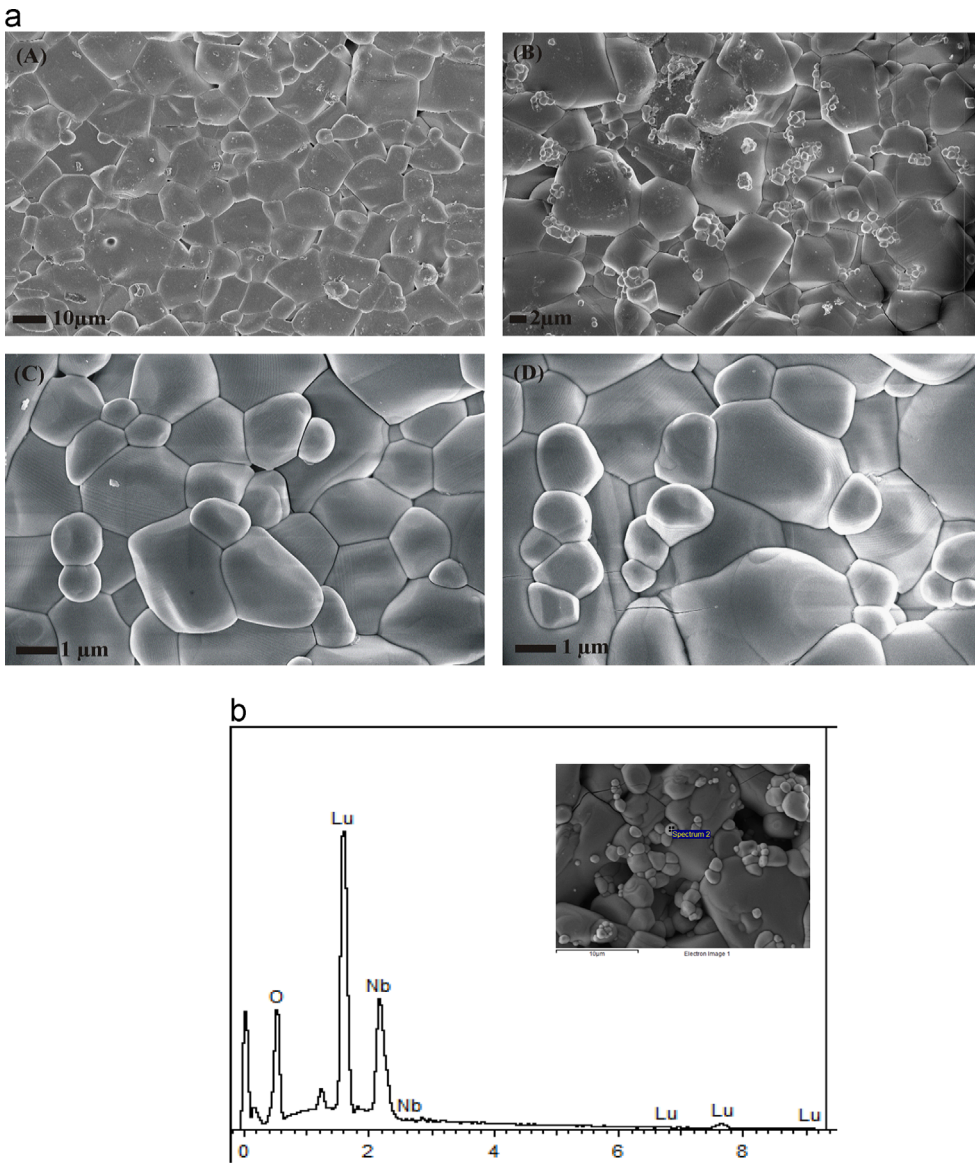

Fig. 2. (a) Microstructure of LN (A) with 2 wt% Sc_2O_3 (B) 4 wt% (C) 6 wt% and (D) 8 wt.% of Lu_2O_3. (b) EDS spectra of LN doped with Lu_2O_3 with corresponding microstructure in the inset.

incorporation of the dopant concentration. The intensities also varied systematically with an increase in dopant concentration. The change in intensities might account for the influence of dopant ions on the (104) and (110) reflection planes.

3.2. Morphology and EDX

The surface morphology of Sc_2O_3 and Lu_2O_3 doped LN are shown in Fig. 2. In case of Sc_2O_3 doped LN, the grain morphology is clear and distinct with well defined grain boundaries. With increase in Sc_2O_3 concentration, micro pores are observed on the surface of grains and at grain boundaries as shown in Fig. 2(a)-(A). In case of Lu_2O_3, small clusters of unreacted Lu_2O_3 grains are distributed more at the grain boundaries which are confirmed from EDS as shown in Fig. 2 (a)-(B). Equiaxed grains of polyhedral shape with different size distribution are observed as shown in fig. 2(a)-(C and D). The grain growth inhibition is observed only at few sites especially at grain boundaries. The segregation of Lu_2O_3 at grain boundaries shows that Lu_2O_3 is only partially reacted with LN. From elemental analysis, it is confirmed that the grains segregated at boundaries are Lu_2O_3. From EDS, it is confirmed that Nb, O, Sc and Lu were present in all the samples with change in atomic wt% according to the stoichiometry. The atomic % of Lu doped LN has been given in Table 1.

3.3. Raman spectra

Minor structural changes cannot be detected from XRD, hence Raman spectroscopy can be used to detect the untraceable phases. Variations in frequency shift, peak broadening and appearance of new peaks from stoichiometric to non stoichiometric LN can be traced out from the obtained spectra [19]. LN exhibits

Table 1
Elemental composition of Lu_2O_3 doped sample.

Element	Weight%	Atomic%	Compound%
Nb	59.79	26.44	85.53
Lu	12.73	2.99	14.47
O	27.49	70.57	

Table 2
Lattice cell parameters and cell volume for all samples.

Sample no.	a=b (Å)	c (Å)	Cell volume [Å]^3
Pure LN	5.16207	13.84830	318.8160
LN+2 wt% Sc_2O_3	5.18683	13.85076	321.6096
LN+4 wt% Sc_2O_3	5.17333	13.88213	322.4076
LN+6 wt% Sc_2O_3	5.19118	13.89745	323.2603
LN+8 wt% Sc_2O_3	5.17750	13.89869	322.8515
LN+2 wt% Lu_2O_3	5.15415	13.86251	318.9093
LN+4 wt% Lu_2O_3	5.15415	13.86251	318.9093
LN+6 wt%Lu_2O_3	5.15530	13.85778	319.0577
LN+8 wt%Lu_2O_3	5.15145	13.85726	318.4891

rhombohedral structure and belongs to C_{3v} space group with two formula units per unit cell. According to group theory calculations, C_{3v} space group has 27 optical vibrational modes which are further categorised as $4A_1+5A_2+9E$ [20].

The A_1 and E modes are Raman active whereas A_2 modes are inactive. In the present study, A_1 modes observed are at 522, 276, 334 and 633 cm^{-1} while E modes are at 155, 180, 238, 265, 325, 371, 431, 582 and 610 cm^{-1}. The modes are assigned according to Y. Repelin et al. [21]. The Raman spectra of Sc_2O_3 and Lu_2O_3 doped LN are given in fig. 3(a) and (b) respectively. From Fig. 3(a) it is noticed that slight disturbances to the Nb–O bonds easily reflect in the broadening of E(TO1) and E(TO3) modes. According to Pauling, the ionic nature of AB bond can be calculated using the difference between the electro-negativities of the two atoms:

$$F(AB) = 1 - exp\left[\frac{-(X_A - X_B)^2}{4}\right] \quad (1)$$

Where X_A and X_B are electro negativities of A and B atoms respectively.

From the above relation, F(Li–O) is 0.79 and F(Nb–O) is 0.73. The ionic character of Li–O bond is greater than Nb–O bond, latter being covalent in nature [22]. Because of this covalency in Nb–O bond, the increase in dopant concentration does not shift these modes appreciably. A maximum shift of 4 cm^{-1} in E (TO3) mode is observed in 6 wt% Sc_2O_3 doped LN sample. The modes A_1(LO1) and A_1(LO2) slowly merge to one peak with an increase in dopant concentration and mostly disappear at $x=8$. Similarly the peaks E(TO4) and A_1(LO3) also merged into one another and broadened completely with increase in concentration. In addition, E(TO5) is shifted to lower frequency side and almost disappeared with

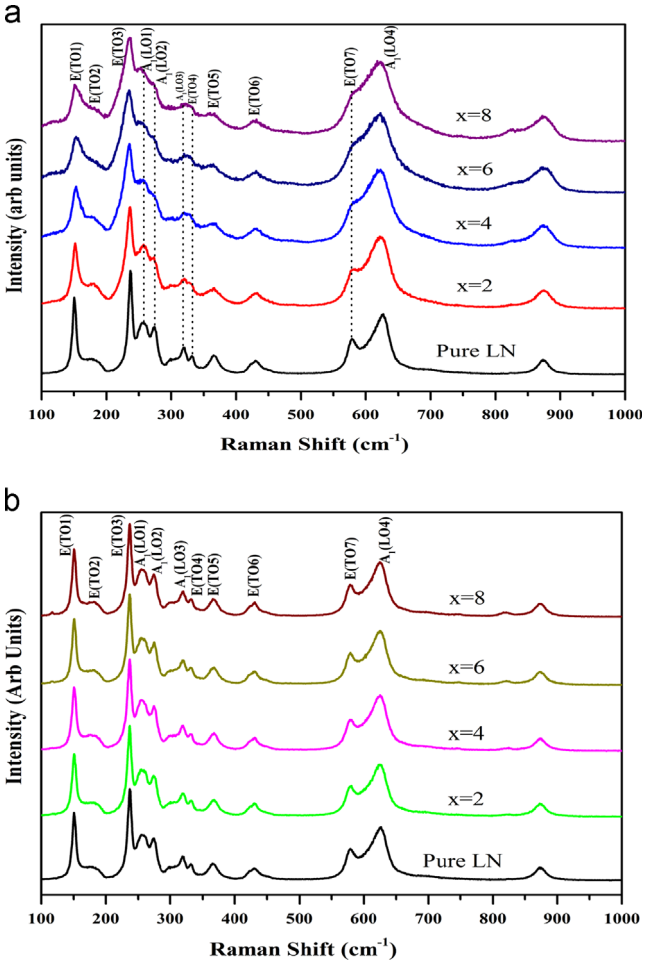

Fig. 3. (a) Raman spectra of Sc_2O_3 doped LN. (b) Raman spectra of Lu_2O_3 doped LN.

an increase in dopant concentration. All the changes in these modes between 400–270 cm^{-1} are arising because of Li cation displacements [23]. Due to the ionic nature of Li–O bond, the evaporation or detachment of Li^{+} from Li-O bond will be more. Due to this reason, the changes like peak broadening and shifting are highly pronounced between 400–270 cm^{-1}.

In case of Lu_2O_3, no peak broadening or peak shifting is observed with increase in dopant concentration as shown in Fig. 3(b). This might be due to two reasons. Firstly, some amount of doped Lu_2O_3 may be inactive with host material LN as discussed in the earlier sections (3.1 and 3.2). Secondly, partially reacted lutetium may replace either Nb^{5+} or Li^{+} sites exactly forming a stable solid solution leading to no structural changes. This is also confirmed from the PL studies which will be discussed in the next section.

3.4. Photoluminescence (PL)

Fig. 4(a) shows PL spectra of LN with different wt% of Sc_2O_3. Bright violet luminescence with emissions at 414 nm and 435 nm upon excitation with an UV light (370 nm) is observed. The luminescence of LN with 6 wt% Sc_2O_3 is 1.5 to 5 times more intense than the remaining (LN with 2, 4 and 8 wt% doped Sc_2O_3). It has a Stokes shift of emission at 415 nm and 436 nm which is quite negligible. Previous reports [24–26] claimed an emission peak at 440 nm which is independent of excitation wavelength. This luminescence is ascribed to the intrinsic electron (Nb^{4+}) and hole (O) recombination at a regular niobate group. The ascending order of concentration quenching is 6 wt% > 8 wt% > 2 wt% > 4 wt%. The concentration quenching was observed at 4 wt% and 8 wt%. It is well known that in polycrystalline samples, grain boundaries act as non radiative centres. In addition, the porosity in the sample may act as scattering centres for the incident light [27]. One of the reasons for the unsystematic variation in intensities of the Sc_2O_3 doped LN is the microstructure.

Fig. 4(b) gives the variation in intensity of the emission peaks of LN with different wt% of Lu_2O_3. Similar trend was observed as in the LN doped with Sc_2O_3. LN with 4 wt% of Lu_2O_3 is exhibiting strong violet luminescence at 415 nm and 436 nm with excitation wavelength of 370 nm. The ascending order of concentration quenching is 4 wt% > 8 wt% > 2 wt% > 6 wt%. Thus, quenching concentration is above 6 wt% Lu_2O_3 and this can be used for strong violet colour emission.

Apart from the violet emission, noticeable green emission is detected with 2 and 4 wt% Sc_2O_3 doped LN as shown in Fig. 5(a). In stoichiometric LN, the blue emission peak centered at 473 nm upon excitation at 289 nm is commonly observed. With increase in dopant wt%, the peak shifted from 473 nm to 505 nm and then

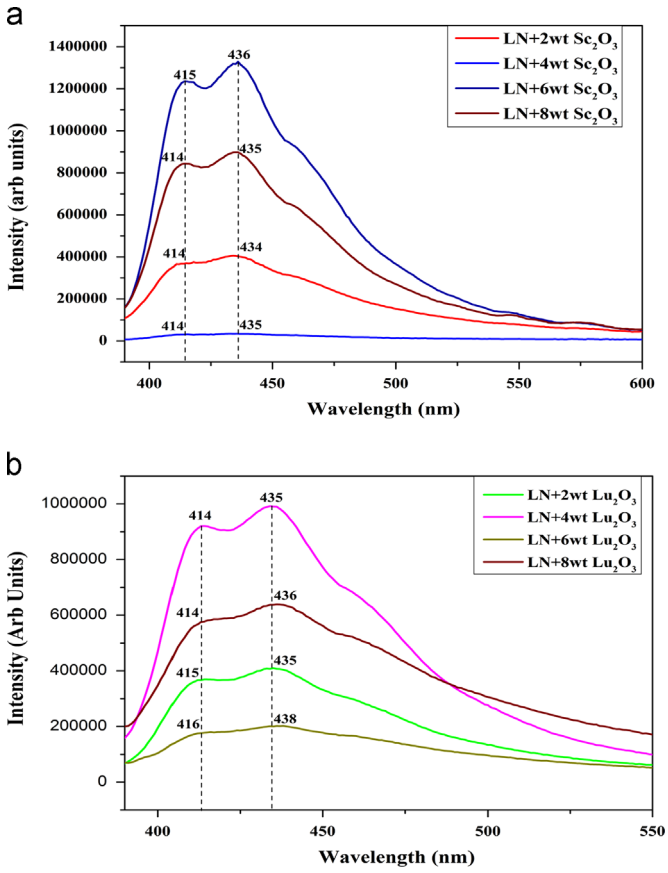

Fig. 4. (a) Variation of intensities in emission spectra of LN with Sc_2O_3 doping. (b) Variation of intensities in emission spectra of LN with Lu_2O_3 doping.

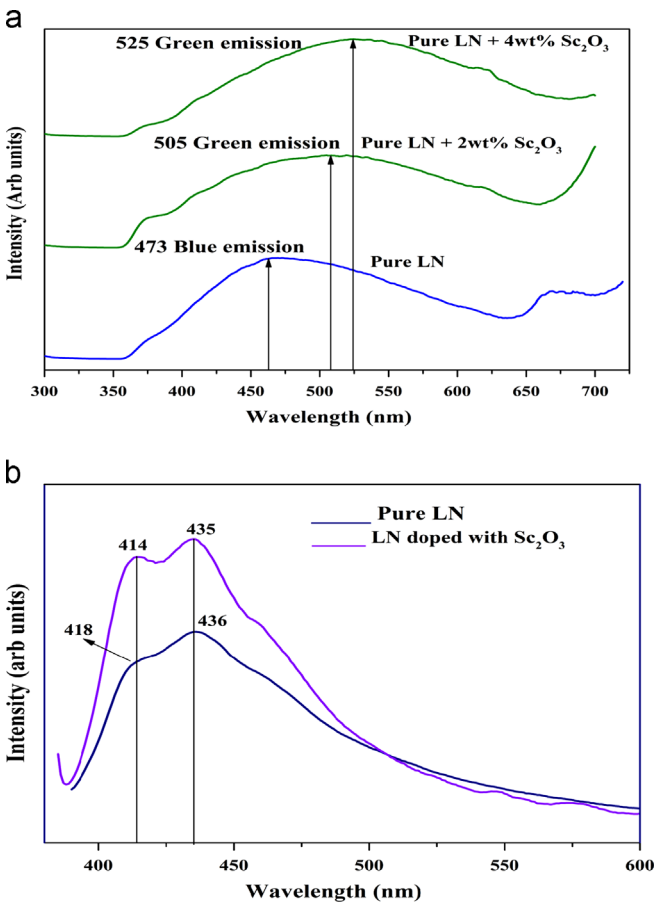

Fig. 5. (a) Emission spectra of LN doped with Sc_2O_3 at an excitation wavelength of 289 nm. (b) Emission spectra of LN doped with Sc_2O_3 at an excitation wavelength of 370 nm. (For interpretation of the references to colour in this figure, the reader is referred to the web version of this article.)

to 525 nm in 2 wt% and 4 wt% Sc_2O_3 doped LN respectively. The emission band at 520nm is attributed to the antisite defects $Nb_{Li}^{\cdots}$ (Kroger–Vink Notation). This is due to the changes occurred as a result of Li:Nb stoichiometry. Moreover, the green emission is observed only in case of 2 and 4 wt% Sc_2O_3 doped LN. This indicates that with increase in Sc_2O_3 concentration, the Nb ions might be replaced with Sc ions or it might have changed the Li sites which are replaced with the Nb as antisite defects. The alteration of niobate group by foreign ion could be responsible for the green light emission [28]. The excess oxygen atoms from Sc_2O_3 may disturb the Nb–O covalency. The Stokes shift from 473 nm to 505 nm may be due to intrinsic defect $Nb_{Li}^{\cdots}$ (Kröger–Vink notation) and substitutional or interstitial defects like $Sc_{Nb}^{''}$, $Sc_{Li}^{\cdots}$. Due to Li evaporation at high sintering temperatures like 1125 °C which is close to its melting temperature 1257 °C, vacancies will be created at Li sites. The quenching concentration is 4 wt% and the green emission coming with the excitation wavelength of 289 nm does not appear with further increase in dopant.

Raman spectra with $x=2$, 4 wt% Sc_2O_3 doped LN (Fig. 3(a)) supports this argument. From previous reports, the green emission is due to the Nb^{5+} ions occupying Li^{+} sites. Thus, the peaks A_1(LO1) and A_1(LO2) corresponding to Li cation displacements and deformation in the Nb–O system also merges into each other as discussed in the earlier section. At $x=2$, 4 the Li^{+} sites may be replaced with Nb^{5+} or Sc^{3+} ions. At $x=6$ wt%, the two peaks merge into each other, which may be an indication of the complete substitution of the foreign ion into the host material. The intensity of emission peak is also much stronger at this particular case. At $x=8$ wt%, the modes A_1(LO1) and A_1(LO2) almost disappear and the corresponding intensity of luminescence peak decreased.

Similar trends were observed in case of Lu_2O_3 doped LN. In case of Lu_2O_3, strong violet emission at 415 nm and 435 nm is observed with an excitation wavelength in the UV region (370 nm). Apart from the violet emission, with an excitation wavelength of 307 nm, an emission peak at 477 nm (blue) is obtained. There is no shift corresponding to the emission peak in blue region (477 nm) with increase in dopant wt%. There are no observable changes with increase in Lu_2O_3 doping. The Lu_2O_3 is only partially reacted with LN. Thus, either the substitution or replacement of Lu^{3+} ion into the host material is not possible. This has been confirmed from fig. 2(a)-(B) where small crystals of Lu_2O_3 along with LN are formed at the grain boundaries. The elemental analysis for these segregated crystals has been confirmed from Table 1.

Fig. 6 gives the transition from blue emission to green emission with change in Sc_2O_3 dopant concentration. The ascending order of the shift shows that the increase in dopant concentration arrived at a quenching level of 4 wt% of Sc_2O_3 after which the green emission disappeared.

4. Conclusion

In summary, LN with different wt% of Sc_2O_3 or Lu_2O_3 was prepared. Changes in intensities of (104) and (110) peaks correspond to the incorporation of Sc^{3+} and Lu^{3+} into LN host material. Unreacted Lu_2O_3 was detected from XRD.

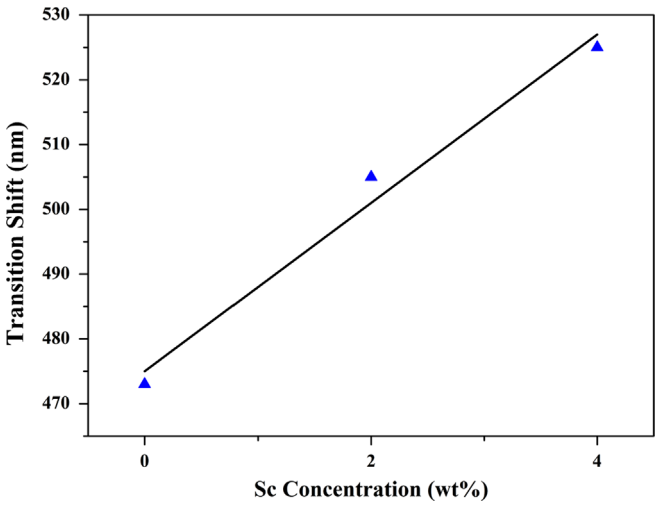

Fig. 6. Shift in transition from blue to green with change in Sc_2O_3 concentration. (For interpretation of the references to colour in this figure legend, the reader is referred to the web version of this article.)

Microstructure from Sc_2O_3 doped LN is found to have uniform grain growth. In case of Lu_2O_3, unreacted Lu_2O_3 is agglomerated as small crystals at the grain boundaries.

Strong violet luminescence is observed for LN doped with Sc_2O_3 and Lu_2O_3 with excitation wavelength in UV region (370 nm). Apart from this, a blue emission at 473 nm with an excitation wavelength of 270 nm is observed in pure LN. This blue emission is red shifted (from 473 nm to 505 nm and then to 525 nm) with increase in Sc_2O_3 concentration. Such shifts are likely to originate from the radiative recombination of electrons and holes. The strong violet luminescence can be attributed to Li and Nb cation displacements as well as antisite defects ($Nb_{Li}^{\cdots}$). The same factors can be considered to be responsible for the defect emissions with Sc_2O_3 and Lu_2O_3 doping. Till date, LN doped with rare earth ions like Pr^{3+}, Dy^{3+}, Ho^{3+}, Er^{3+}, Tb^{3+}, Nd^{3+} and Tm^{3+} have exhibited blue, green, red, yellow and violet up conversion emissions. But the observed strong violet luminescence with UV excitation of Sc_2O_3 and Lu_2O_3 doped polycrystalline LN opens a possibility to explore this composition as a luminescent material in converting UV energy to visible light in the violet region.

Acknowledgements

T. Anil is thankful to Prof. TPR and Mr.Gupta for helping in recording luminescence spectra. Also authors acknowledge DST and UGC for providing XRD, FE-SEM and Raman spectrometery.

References

[1] Yongfa Kong, Shengqing Wu, Shinguo Liu, Shaolin Chen, Jingjun Xu, Fast photorefractive response and high sensitivity of Zr and Fe codoped $LiNbO_3$ crystals, Applied Physics Letters 92 (2008) 251107.

[2] Debasish Mohanty, Girija S. Chaubey, Amin Yourdkhani, Shiva Adireddy, Gabriel Caruntu, John B. Wiley, Synthesis and

piezoelectric response of cubic and spherical $LiNbO_3$ nanocrystals, RSC Advances 2 (2012) 1913–1916.
[3] S. Dunn, D. Tiwari, Influence of ferroelectricity on the photoelectric effect of $LiNbO_3$, Applied Physics Letters 93 (2008) 092905.
[4] Shohei Tachi, Ken-ichi Kakimoto, Isao Kagomiya, Temperature dependence of elastic and piezoelectric properties of lead-free (Li, Na, K) NbO_3 ceramics, Ceramics International 38 (Suppl. 1) (2012) S311–S314 (The 7th Asian meeting on Electroceramics (AMEC-7) in conjuction with the 7th Asian meeting on Ferroelectricity (AMF-7).
[5] H. Lu, B. Sadani, N. Courjal, G. Ulliac, N. Smith, Enhanced electro-optical Lithium niobate photonic crystal wire waveguide on a smart cut thin film, Optics Express 20 (3) (2012) 2974–2981.
[6] Ch.N. Rao, Anoopam Bharadwaj, Suwarna Datar, S.N. Kale, Lithium niobate nanoparticulate clad on the core of single mode optical fibre for temperature and magnetic field sensing, Applied Physics Letters 101 (2012) 043102.
[7] K.K. Shung, J.M. Cannata, Q.F. Zhou, Piezoelectric materials for high frequency medical imaging applications: a review, Journal of Electro ceramics 19 (2007) 139–145.
[8] R.N. Zhukov, A.S. Bykon, D.A. Kiselev, M.D. Malinkovich, Yu. N. Parkhomenko, Piezoelectric properties and surface potential behaviour in $LiNbO_3$ thin films grown by the RF magnetron sputtering, Journal of Alloys and Compounds (2013) (In press-corrected proof).
[9] Yunhua Wang, Biao Wang, Dong Wu, Shaopeng Lin, Zifan Zhou, Yonzhong Zhu, Optical properties of Sm^{3+} doped Mg:$LiNbO_3$ and Zn:$LiNbO_3$ single crystals, Optical Materials 34 (2012) 845–849.
[10] T. Jardiel, A.C. Caballero, M. Marin Dobrincic, E. Cantelar, F. Cusso, Bottom-up synthesis of up-converting submicron-sized Er^{3+} doped $LiNbO_3$ particles, Materials Chemistry and Physics 135 (2012) 676–680.
[11] Zhaopeng Xu, Jie Gong, Aihua Li, Ying Han, Yaping Luo, Spectroscopic properties of near stiochiometric In:Er:$LiNbO_3$ crystals, Journal of Luminescence 135 (2013) 10–14.
[12] Lili Xing, Rui Wang, Wei Xu, Yannan Qian, Yanling Xu, Chunhui Yang, Xinrong Liu, Upconversion white-Light emission in Ho^{3+}/Yb^{3+}/Tm^{3+} codoped $LiNbO_3$ polycrystals, Journal of Luminescence 132 (2012) 1568–1574.
[13] A. Brenier, G. Boulon, New criteria to choose the best Yb^{3+} doped laser crystals, Europhysics letters 55 (5) (2001) 647.
[14] Daniele Gozzi, Alessandro Latini, Daniele Carta, Anna Corrias, Andreas Falqui, Lanthanide-doped scandia and yttria cathodoluminescence films: a comparitive study, Chemistry of Materials 20 (2008) 5666–5674.
[15] R. Krsmanovic, O.I. Lebedev, A. Speghini, M. Bettinelli, S. Polizzi, G. Van Tendeloo, Structural and Luminescence investigation on gadolinium gallium garnet nanocrystalline powders prepared by solution combustion synthesis, Nanotechnology 18 (2007) 325604.
[16] Xiao Lu, Benxue Jiang, Jiang Li, Wenbin Liu, Liang Wang, Xuewei Ba, Chen Hu, Binglong Liu, Yubai Pan, Synthesis of highly sinterable Yb:Sc_2O_3 nanopowders for transparent ceramic, Ceramics International 39 (4) (2013) 4695–4700.
[17] R. Burlton, R. Moncorge, G. Boulon, Visible and infrared luminescence properties of Er^{3+} doped Sc_2O_3:$LiNbO_3$ crystal fibers, Journal of Luminescence, 72–74 (1997) 135–138.
[18] A.N. Gruzintsev, G.A. Emelchenko, Yu.V. Yermolayeva, V.M. Masalov, A.V. Tolmachev, Spontaneous and stimulated red luminescence of Lu_2O_3: Eu nanocrystals, Physics of The Solid State 53 (6) (2011) 1263–1268.
[19] N.V. Sidorov, M.N. Palatnikov, V.T. Gabrielyan, P.G. Chufyrev, V.T. Kalinnikov, Raman spectra and structural perfection of nominally pure lithium niobate crystals, Inorganic Materials 43 (1) (2007) 60–67.
[20] Greg Stone, Brian Knorr, Venkatraman Gopalan, Volkmar Dierolf, Frequency shift of Raman modes due to an applied electric field and domain inversion in $LiNbO_3$, Physical Review B 84 (2011) 134303.
[21] Y. Repelin, E. Husson, F. Bennani, C. Proust, Raman spectroscopy of lithium niobate and lithium tantalate: force field calculations, Journal of Physics and Chemistry of solids 60 (1999) 819–825.
[22] S. Kar, R. Bhatt, V. Shukla, R.K. Choubey, P. Sen, K.S. Batwal, Optical behaviour of VTE treated near stoichiometric $LiNbO_3$ crystals, Solid State Communications 137 (2006) 283–287.
[23] P. Hermet, M. Veithen, First-principles calculations of the nonlinear optical susceptabilities and Raman scattering spectra of lithium niobate, Journal of Physics Condensed Matter 19 (2007) 456202.
[24] M. Wiegel, M.H.J. Emond, E.R. Stobbe, G. Blasse, Luminescence of alkali niobates and tantalates, Journal of Physics and Chemistry of solids 55 (8) (1994) 773–778.
[25] V. Pankratov, L. Grigorjeva, D. Millers, G. Corradi, K. Polgar, Luminescence of ferroelectric crystals: $LiNbO_3$ and $KNbO_3$, Ferroelectrics 239 (2000) 241–250.
[26] D.M. Krol, G. Blasse, R.C. Powell, The influence of the Li/Nb ratio on the luminescence properties of $LiNbO_3$, Journal of Chemical Physics 73 (1980) 163.
[27] Hyungjin Bang, Shinichi Morishima, Junji Sawahata, Jongwon Seo, Mikio Takiguchi, Masato Tsunemi, Katsuhiro Akimoto, Masaharu Nomura, Concentration quenching of Eu-related luminescence in Eu-doped GaN, Applied Physics Letters 85 (2004) 2.
[28] K.K. Wong, Properties of Lithium Niobate, INSPEC publication, London, UK, 2002 (ISBN 0852967993).